Quantized lattice dynamic effects on the Peierls transition of the extended Hubbard-Peierls model

Christopher J. Pearson,[1] William Barford,[1,*] and Robert J. Bursill[2]

[1]*Department of Chemistry, Physical and Theoretical Chemistry Laboratory, University of Oxford, Oxford OX1 3QZ, United Kingdom*

[2]*School of Physics, University of New South Wales, Sydney, New South Wales 2052, Australia*

(Received 28 October 2010; revised manuscript received 10 March 2011; published 4 May 2011)

The density matrix renormalization group method is used to investigate the Peierls transition for the extended Hubbard model coupled to quantized phonons. Following our earlier work on spin-Peierls systems, we use a phonon spectrum that interpolates between a gapped, dispersionless (Einstein) limit and a gapless, dispersive (Debye) limit to investigate the entire frequency range. A variety of theoretical probes are used to determine the quantum phase transition, including energy gap crossing, a finite-size scaling analysis, and bipartite quantum entanglement. All these probes indicate that a transition of Berezinskii-Kosterlitz-Thouless type is observed at a nonzero electron-phonon coupling g_c for a nonvanishing electron-electron interaction. An extrapolation from the Einstein limit to the Debye limit is accompanied by an increase in g_c for a fixed optical ($q = \pi$) phonon gap. We therefore conclude that the dimerized ground state is more unstable with respect to Debye phonons, with the introduction of phonon dispersion renormalizing the effective electron-lattice coupling for the Peierls-active mode. By varying the Coulomb interaction U, we observe a generalized Peierls transition, intermediate between the uncorrelated ($U = 0$) and spin-Peierls ($U \to \infty$) limits, where U is the Hubbard Coulomb parameter. Using the extended Hubbard model with Debye phonons, we investigate the Peierls transition in *trans*-polyacetylene and show that the transition is close to the critical regime.

DOI: 10.1103/PhysRevB.83.195105 PACS number(s): 71.10.Fd, 71.30.+h, 71.38.−k

I. INTRODUCTION

Low-dimensional electronic materials are known to be highly susceptible to electron-phonon-driven structural distortions. Over half a century ago, Peierls demonstrated that a one-dimensional (1D) metallic system can support a periodic modulation in the equilibrium positions of the lattice ions.[1] For the case of a half-filled band, the broken-symmetry phase is commensurate with the lattice, resulting in a doubling of the unit cell of the ground state (GS). Since the dimerization opens a gap at the Fermi surface, the Peierls process transforms the metal to a dielectric phase, with the increase in lattice energy associated with the permanent distortion being offset by the reduction in electronic kinetic energy. Spontaneous dimerization has been noted in many quasi-1D materials, ranging from organic conjugated polymers[2,3] and charge-transfer salts[4] to inorganic blue bronzes[5] and *MX* chains.[6]

The Peierls instability is well understood in the *static lattice* limit for which the frequency ω_π of the Peierls-active mode is taken to be much smaller than the electron hopping integral t. In the adiabatic phonon limit, the GS is known to have a broken-symmetry staggered dimerization for arbitrary electron-phonon coupling. Experimentally, such behavior was first observed in the 1970s for the organic compounds of the TTF and TCNQ series.[4] For many quasi-one-dimensional materials, however, the zero-point fluctuations of the phonon field are comparable to the amplitude of the Peierls distortion.[7–9] Lattice dynamic (quantum phonon) effects should therefore be included in a full theoretical treatment of Peierls-distorted systems.

Likewise, interest in models of *spins* coupled dynamically to phonons increased significantly when it was shown that the first inorganic spin-Peierls (SP) compound[10] $CuGeO_3$ exhibits no clear scale separation between magnetic and phononic energies. Moreover, in contrast to the organic SP materials, no phonon softening is observed at the transition. SP physics, then, is plainly in the nonadiabatic regime.

Using the density matrix renormalization group (DMRG), it has been demonstrated that quantum fluctuations destroy the Peierls state for small, nonzero couplings in both the spinless[11] and spin-$\frac{1}{2}$ (Ref. 12) Holstein models at half filling. Analogous results for the XY SP model with gapped, dispersionless (Einstein) phonons were obtained by Caron and Moukouri,[13] using finite-size scaling analysis of the spin gap to demonstrate a power law relating the critical coupling and the Peierls-active phonon frequency: $g_c^{XY} \sim \omega_\pi^{0.7}$. Citro *et al.*[14] used a renormalization group (RG) treatment of the bosonized Heisenberg-SP model to demonstrate similar behavior in the antiadiabatic phonon regime ($\omega_\pi / J \gg 1$). In general, for models with sufficiently large Einstein frequency, gapped phonon degrees of freedom can always be integrated away to generate a low-energy effective-fermion Hamiltonian characterized by instantaneous, nonlocal interactions.[15,16]

Gapless, dispersive (Debye) phonons were found by the present authors to destabilize the broken-symmetry GS of the Heisenberg-SP chain,[17] which maps to a spinless-fermion-Peierls chain under Jordan-Wigner (JW) transformation. By interpolating between the Einstein- and Debye-phonon limits, the spin-Peierls phase was shown to be *more* unstable with respect to dispersive lattice degrees of freedom. For the Su-Schrieffer-Heeger (SSH) model, Fradkin and Hirsch undertook an extensive study of spin-$\frac{1}{2}$ ($n = 2$) and spinless ($n = 1$) fermions using world-line Monte Carlo simulations.[18] In the antiadiabatic limit (i.e., vanishing ionic mass M), they mapped the system onto an n-component Gross-Neveu model, known to exhibit long-ranged dimerization for arbitrary coupling for $n \geqslant 2$ (although not for $n = 1$). For $M > 0$ an RG analysis indicates the low-energy behavior of the $n = 2$ model to be

governed by the zero-mass limit of the theory, indicating that the spinful model presents a dimerized GS for arbitrarily weak e-ph couplings.[19]

Although of theoretical interest, independent-electron models are not sufficient to give a quantitative account of the properties of physical systems exhibiting a Peierls distortion—for that, electron-electron (e-e) interactions must be included. The interplay between e-e and electron-phonon (e-ph) interactions results in an extremely rich phase diagram of broken-symmetry GSs, each supporting a range of low-energy electron-lattice excitations: solitons, polarons, lattice "breathers," etc.[2,3] For the half-filled Hubbard model, repulsive on-site interactions in the charge sector ($U > 0$) give rise to the opening of a charge gap Δ_ρ and, in the absence of e-ph couplings, the system is a Mott insulator (MI): a critical dielectric phase exhibiting algebraically decaying spin-spin correlations.[20] Hence, the transition from the MI to the Peierls insulator (PI) phase is accompanied only by the generation of a spin gap Δ_σ, the charge gap having arisen by virtue of mutual electronic repulsions. Longer-range e-e interactions, e.g., next-nearest neighbor terms (V), can destroy the Mott state, however, and are expected to influence the MI-PI transition. Even in the absence of lattice degrees of freedom, the phase diagram of the simplest half-filled extended Hubbard model is still controversial: its behavior close to the $U = 2V$ line has attracted significant attention, with a Peierls-like bond-ordered GS predicted to exist.[21]

Sengupta *et al.*,[22] using the extended Hubbard model coupled to Einstein *bond* phonons, demonstrated the destruction of the PI below a nonzero value of the e-ph coupling, in agreement with earlier independent-electron treatments. Work by Zimanyi *et al.*[24] on one-dimensional models with both e-e and e-ph interactions indicated the development of a spin gap provided the combined backscattering amplitude $g_1^T = g_1(\omega) + \tilde{g}_1(\omega) < 0$, where $g_1(\omega)$ is the contribution from e-e interactions and $\tilde{g}_1(\omega) < 0$ is the e-ph contribution in the notation of Ref. 24. Hence, for the pure *spinful* SSH model ($U = V = 0$), $g_1 = 0$ and $g_1^T < 0$ for any nonzero e-ph coupling, implying a Peierls GS for arbitrary e-ph coupling, in agreement with the earlier Monte Carlo results.[18] It should be noted, however, that a dimerized state was also predicted for $g_c = 0^+$ in the spin-$\frac{1}{2}$ Holstein model, for which later large-scale calculations indicated a nonzero critical coupling.[25]

In this paper we examine the influence of gapless, dispersive phonons on the GS of the extended Hubbard-Peierls (EHP) chain. We explicitly probe the MI-PI transition, studying the model as a function of the electron-phonon interaction g, Coulomb interactions U and V, and phonon frequency ω_π. In all cases we consider a half-filled band. Since the parameter space of this model is rather large, we restrict our study to a physically reasonable ratio $U/V = 4$ of the e-e parameters for the full phonon-frequency range. This ratio of U to V is widely accepted to best model *trans*-polyacetylene (PA) via the extended Hubbard model. We return to a discussion of *trans*-PA in Sec. III H. In addition, we investigate the model for $\omega_\pi/t = 1$ for all values of U. The $U \to \infty$ limit is of particular relevance to our earlier work,[17] since in the limit of large Hubbard interactions, the EHP Hamiltonian maps onto the quantum Heisenberg-Peierls antiferromagnet. However, for most polyenes, the Coulomb interactions are not large enough to justify the spin model.[26] We also note that in the limit of vanishing phonon frequency ($M \to \infty$) the model maps onto the extensively studied classical adiabatic chain.

That the dispersive-phonon EHP model is yet to receive the same level of attention as its gapped, dispersionless counterpart is due in part to the presence of hydrodynamic modes, resulting in logarithmically increasing vibrational amplitudes with chain length. To this end, acoustic phonons have been assumed to decouple from the low-energy electronic states involved in the Peierls instability, motivating the retention of only the optical phonons close to $q = \pi$.[18,22,24] In this regard, optical phonons have been expected to be equivalent to fully quantum mechanical SSH phonons. Even for pure Einstein phonons, however, Wellein, Fehske, and Kampf[27] found the singlet-triplet excitation to be strongly renormalized when phonons of all wave number are taken into account, the restriction to solely the $q = \pi$ modes leading to a substantial overestimation of the spin gap. Physically, this implies that the spin-triplet excitation is accompanied by a local distortion of the lattice, necessitating a multiphonon mode treatment of the ionic degrees of freedom. Our recent work on the SP model has indicated that truncating the Debye-phonon spectrum, leaving only those modes which couple directly to the Peierls phase, is not physically quantitatively reasonable.

We use the DMRG technique[28] to numerically solve the EHP model for $t = U/4 = V$ with a generalized gapped, dispersive phonon spectrum. The phonon spectrum interpolates between a gapped, dispersionless (Einstein) limit and a gapless, dispersive (Debye) limit. We proceed by considering a system of tightly bound Wannier electrons dressed with pure Einstein phonons for which we observe a Berezinskii-Kosterlitz-Thouless (BKT) quantum phase transition at a nonzero electron-lattice coupling. Progressively increasing the Debye character of the phonon dispersion (at given optical phonon adiabaticity) results in an increase in the critical value of the e-ph coupling, with the transition remaining in the BKT universality class (see Sec. III C). These findings are corroborated by an array of independent verifications: energy-gap crossings in the spin excitation spectra (see Sec. III A), finite-size scaling of the spin gap (see Sec. III B), and quantum bipartite entanglement (see Sec. III D). Our approach here is equivalent to that described in Ref. 17 to investigate the BKT transition in the spin-Peierls model. In addition, we use conformal invariance to show that the dimerization is consistent with a transition of the BKT type (see Sec. III E).

We note that earlier DMRG investigations of the EHP Hamiltonian with Debye phonons indicated a dimerized GS for arbitrary coupling.[29] This conclusion was based on the behavior of the staggered phonon order parameter, which we have since shown to be an unreliable signature of the transition.[17] We therefore pursue alternative characterizations of the Peierls state in this work.

In the next section we describe the model, before discussing our results in Sec. III.

II. THE MODEL

The extended Hubbard-Peierls Hamiltonian is defined by

$$H = H_{e\text{-}e} + H_{e\text{-ph}} + H_{\text{ph}}. \tag{1}$$

$H_{e\text{-}e}$ describes the electronic degrees of freedom,

$$H_{e\text{-}e} = -t\sum_{l,\sigma}(c^{\dagger}_{l\sigma}c_{l+1\sigma} + c^{\dagger}_{l+1\sigma}c_{l\sigma}) + U\sum_{l}\left(N_{l\uparrow} - \frac{1}{2}\right)\left(N_{l\downarrow} - \frac{1}{2}\right) + V\sum_{l}(N_l - 1)(N_{l+1} - 1),$$

and $H_{e\text{-ph}}$ the e-ph coupling,

$$H_{e\text{-ph}} = -\alpha\sum_{l,\sigma}(u_{l+1} - u_l)(c^{\dagger}_{l\sigma}c_{l+1\sigma} + c^{\dagger}_{l+1\sigma}c_{l\sigma}). \tag{2}$$

Here, $N_{l\sigma} = c^{\dagger}_{l\sigma}c_{l\sigma}$, where $c^{\dagger}_{l}$ ($c_{l\sigma}$) creates (annihilates) a spin-σ electron at Wannier site l of an N-site one-dimensional (1D) lattice, u_l is the displacement of the lth ion from equilibrium, α is the e-ph coupling parameter, and U and V are the on-site and nearest neighbor Coulomb interactions, respectively.

H_{ph} describes the lattice degrees of freedom. In the Einstein model the ions are decoupled,

$$H^{E}_{\text{ph}} = \sum_{l}\frac{P^2_l}{2M} + \frac{1}{2}K\sum_{l}u^2_l. \tag{3}$$

In the Debye model, however, the ions are coupled to nearest neighbors,

$$H^{D}_{\text{ph}} = \sum_{l}\frac{P^2_l}{2M} + \frac{1}{2}K\sum_{l}(u_{l+1} - u_l)^2. \tag{4}$$

For the Einstein phonons it is convenient to introduce phonon creation, $b^{\dagger}_{l}$, and annihilation operators, b_l, for the lth site via

$$u_l = \left(\frac{\hbar}{2M\omega_X}\right)^{1/2}(b^{\dagger}_{l} + b_l) \tag{5}$$

and

$$P_l = i\left(\frac{M\hbar\omega_X}{2}\right)^{1/2}(b^{\dagger}_{l} - b_l), \tag{6}$$

where

$$\omega_X = \omega_E = \sqrt{K/M} \equiv \omega_b. \tag{7}$$

Making these substitutions in Eqs. (2) and (3) gives

$$H_{e\text{-ph}} = -t\sum_{l}\left[1 + g_E\left(\frac{\hbar\omega_E}{t}\right)^{1/2}(B_l - B_{l+1})\right] \times (c^{\dagger}_{l\sigma}c_{l+1\sigma} + \text{H.c.}) \tag{8}$$

and

$$H^{E}_{\text{ph}} = \hbar\omega_E\sum_{l}\left(b^{\dagger}_{l}b_l + \frac{1}{2}\right), \tag{9}$$

where $B_l = \frac{1}{2}(b^{\dagger}_{l} + b_l)$ is the dimensionless phonon displacement and

$$g_E = \left(\frac{\alpha^2}{M\omega^2_E t}\right)^{1/2} = \left(\frac{\alpha^2}{Kt}\right)^{1/2} \tag{10}$$

is the dimensionless e-ph coupling parameter.

For the Debye phonons we introduce phonon creation and annihilation operators defined by Eqs. (5) and (6) where

$$\omega_X = \omega_D = \sqrt{2K/M} \equiv \sqrt{2}\omega_b. \tag{11}$$

Making these substitutions in Eqs. (2) and (4) gives

$$H_{e\text{-ph}} = -t\sum_{l}\left[1 + g_D\left(\frac{\hbar\omega_D}{t}\right)^{1/2}(B_l - B_{l+1})\right] \times (c^{\dagger}_{l\sigma}c_{l+1\sigma} + \text{H.c.}) \tag{12}$$

and

$$H^{D}_{\text{ph}} = \hbar\omega_D\sum_{l}\left(b^{\dagger}_{l}b_l + \frac{1}{2}\right) - \hbar\omega_D\sum_{l}B^{\dagger}_{l+1}B_l, \tag{13}$$

where

$$g_D = \left(\frac{\alpha^2}{M\omega^2_D t}\right)^{1/2} = \left(\frac{\alpha^2}{2Kt}\right)^{1/2}. \tag{14}$$

H^{D}_{ph} may be diagonalized by a Bogoliubov transformation[30] to yield

$$H^{D}_{\text{ph}} = \hbar\sum_{q}\omega_D(q)\beta^{\dagger}_{q}\beta_q, \tag{15}$$

where $\omega_D(q)$ is the dispersive, gapless phonon spectrum,

$$\omega_D(q) = \sqrt{2}\omega_D\sin\left(\frac{q}{2}\right) \tag{16}$$

for phonons of wave vector q.

We now introduce a generalized electron-phonon model with a dispersive, gapped phonon spectrum, via

$$H_{e\text{-ph}} = t\sum_{l}\left[1 + g\left(\frac{\hbar\omega_\pi}{t}\right)^{1/2}(B_l - B_{l+1})\right] \times (c^{\dagger}_{l\sigma}c_{l+1\sigma} + \text{H.c.}) \tag{17}$$

and

$$H_{\text{ph}} = \hbar(\omega_E + \omega_D)\sum_{l}\left(b^{\dagger}_{l}b_l + \frac{1}{2}\right) - \hbar\omega_D\sum_{l}B^{\dagger}_{l+1}B_l. \tag{18}$$

Again, Eq. (18) may be diagonalized to give

$$H_{\text{ph}} = \hbar\sum_{q}\omega(q)\beta^{\dagger}_{q}\beta_q + \text{ const}, \tag{19}$$

where

$$\omega(q) = (\omega_E + \omega_D)\left[1 - \left(\frac{\omega_D}{\omega_E + \omega_D}\right)\cos q\right]^{1/2} \tag{20}$$

is the generalized phonon dispersion, as shown in Fig. 1. The $q = 0$ phonon gap frequency is

$$\omega(q = 0) \equiv \omega_0 = [\omega_E(\omega_E + \omega_D)]^{1/2} \tag{21}$$

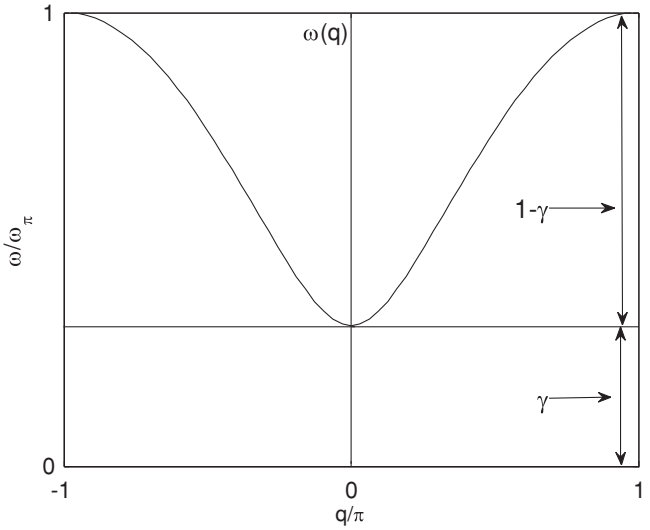

FIG. 1. Generalized phonon dispersion, defined in Eq. (20). $(1-\gamma)\omega_\pi$ is the phonon "bandwidth" (which vanishes in the Einstein limit), while $\gamma\omega_\pi$ is the phonon "mass gap" (which vanishes in the Debye limit).

and the $q=\pi$ optical phonon frequency is

$$\omega(q=\pi)\equiv\omega_\pi=[(\omega_E+\omega_D)(\omega_E+2\omega_D)]^{1/2}. \quad (22)$$

We now define the dispersion parameter γ as

$$\gamma=\omega_0/\omega_\pi. \quad (23)$$

γ is a mathematical device that interpolates the generalized model between the Einstein ($\gamma=1$) and Debye ($\gamma=0$) limits for a fixed value of the $q=\pi$ phonon frequency ω_π. The dimensionless spin-phonon coupling g as well as ω_π/t and γ are the independent parameters in this model. ω_E and ω_D, on the other hand, are determined by Eqs. (21), (22), and (23).

The generalized model can be mapped onto the physical Einstein and Debye models by the observation that in the Einstein limit

$$\begin{aligned}\omega_\pi&=\omega_E\equiv\omega_0;\\ g&=g_E,\end{aligned} \quad (24)$$

while in the Debye limit

$$\begin{aligned}\omega_\pi&=\sqrt{2}\omega_D\equiv 2\omega_0;\\ g&=g_D/2^{1/4}.\end{aligned} \quad (25)$$

The introduction of a generalized phonon Hamiltonian avoids the problems associated with hydrodynamic modes and places a criterion on the reliability of the gap-crossing characterization of the critical coupling (as described in Sec. III A). Starting from the extended Hubbard-Peierls Hamiltonian in the Einstein limit ($\gamma=1$), the effect of dispersive lattice fluctuations can be investigated via a variation of γ. The Debye limit is then found via an extrapolation of $\gamma\to 0$.

We note that the EHP model is invariant under the particle-hole transformation $c^\dagger_{i\sigma}\to(-1)^i c_{i\bar{\sigma}}$. This so-called charge-conjugation symmetry is exact for π-electron models but it is only an approximate symmetry for conjugated polymers and is strongly violated for systems possessing heteroatoms. Nevertheless, for the EHP model at half filling it is expedient to employ particle-hole symmetry to distinguish between different types of singlet excitations, as described in Sec. III A.

The many-body problem is solved using the density matrix renormalization group method[28] with periodic boundary conditions throughout. Our implementation of the DMRG method, including a description of the adaptation of the electron-phonon basis and convergence, is outlined in Refs. 9, 17, and 29.

III. RESULTS AND DISCUSSION

A. Gap crossing

Since both the MI and PI possess a nonvanishing charge gap Δ_ρ, spectroscopy of the spin excitation sector must be used to characterize the GS phase. For the Einstein model with a nonvanishing value of ω_E, the critical e-ph coupling g_c may be determined using the gap-crossing method of Okamoto and Nomura[31] (as illustrated in Fig. 2 of Ref. 17). If the N-site system is a MI exhibiting quasi-long-range order for $0\leqslant g\leqslant g_c(N)$, the lowest spin-sector excitation is to a triplet state, i.e., $\Delta_{\rm st}<\Delta_{\rm ss}$ and $\lim_{N\to\infty}\Delta_{\rm st}=\lim_{N\to\infty}\Delta_{\rm ss}=0$, where $\Delta_{\rm st}$ and $\Delta_{\rm ss}$ are the triplet and singlet gaps, respectively. Conversely, for $g>g_{\rm c}(N)$, the system is dimerized with a doubly degenerate singlet GS in the asymptotic limit (corresponding to the translationally equivalent A and B phases), while the lowest-energy triplet excitation is gapped. However, for finite systems the two equivalent dimerization phases mix via quantum tunneling, and now $\Delta_{\rm ss}<\Delta_{\rm st}$, with $\lim_{N\to\infty}\Delta_{\rm ss}=0$ and $\lim_{N\to\infty}\Delta_{\rm st}\equiv\Delta_\sigma>0$. The gap-crossing condition $\Delta_{\rm st}=\Delta_{\rm ss}$ therefore defines the finite-lattice crossover coupling $g_{\rm c}(N)$. The singlet gap with which we are concerned here is the lowest singlet (covalent) excitation with the same, i.e., *positive*, particle-hole symmetry as the GS. Conversely, the charge gap Δ_ρ is the lowest singlet (ionic) excitation with *negative* particle-hole symmetry, i.e., $\Delta_\rho\equiv\Delta^-_{\rm ss}$. For small $g>g_{\rm c}$, $\Delta_{\rm ss}\equiv\Delta^+_{\rm ss}<\Delta^-_{\rm ss}$. Since we are concerned only with the spin-excitation sector, we hereafter refer to the bulk-limit spin gap Δ_σ as Δ.

For the Debye model, however, the gap-crossing method fails because of the $q\to 0$ phonons that form a gapless vibronic progression with the GS. The hybrid spectrum (shown in Fig. 1) allows us to extrapolate from the pure Einstein limit to the Debye limit, as the lowest vibronic excitation is necessarily $\gamma\omega_\pi$. Provided that $\Delta_{\rm ss}<\omega(q=0)\equiv\gamma\omega_\pi$, the gap-crossover method unambiguously determines the nature of the GS. We can confidently investigate Eq. (1) for $(0.1\leqslant\gamma\leqslant 1)$ with $\omega_\pi/t\in[1,10]$, thereby determining $g_{\rm c}(N,\gamma)$. A polynomial extrapolation of $1/N\to 0$ generates the bulk-limit critical coupling $g_{\rm c}^\infty$ for a given γ (as illustrated in Fig. 2 of Ref. 17). A subsequent polynomial extrapolation determines the $\gamma=0$ (Debye) limit. A phase diagram for the EHP chain found in this way is shown in Fig. 2. Notice that for a fixed ω_π the critical coupling is larger for the Debye model than for the Einstein model, showing that the quantum fluctuations from the $q<\pi$ phonons (as well as the $q=\pi$ phonon) destablize the Peierls state, in agreement with our earlier work on spin-phonon systems. We give a qualitative explanation for this result in Sec. III F.

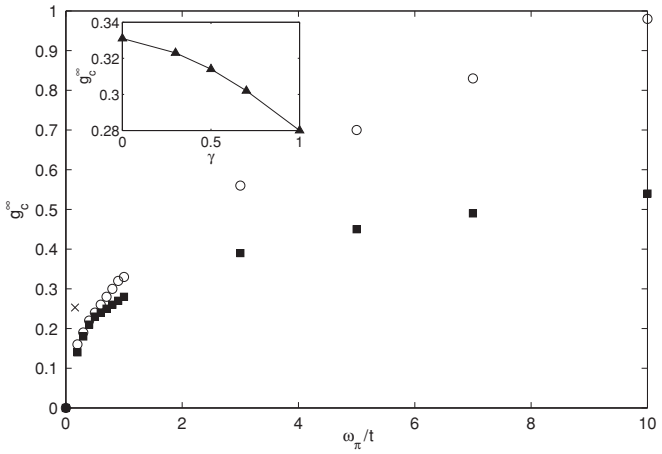

FIG. 2. Phase diagram in the g_c^∞-ω_π plane for the infinite EHP chain for the Einstein limit (squares); extrapolation to $\gamma = 0$ generates the Debye limit (circles). The cross (×) indicates the parameters relevant for *trans*-polyacetylene (see Sec. III H). Inset: Variation of g_c^∞ with γ for $\omega_\pi/t = 1$. In all cases, $V = U/4 = t$.

Following Caron and Moukouri,[13] as well as our more recent work on the Heisenberg-SP model, we propose a general power law, relating the bulk-limit critical coupling to ω_π for a given γ of the EHP model,

$$g_c^\infty(\omega_\pi/t,\gamma) = \beta(\gamma)(\omega_\pi/t)^{\eta(\gamma)}. \tag{26}$$

The infinite-chain values of β, η, and g_c^∞ are given in Table I. We observe a nonzero critical coupling for all phonon-dispersion regimes γ, with the absolute value of g_c^∞ increasing as $\gamma \to 0$. We also find the power relation to be robust, extending well into the adiabatic regime ($\omega_\pi/t \ll 1$).

We next consider the role of Coulomb repulsion by varying the on-site interaction U subject to $U/V = 4$. In the adiabatic limit, the amplitude of the bond alternation initially increases with Coulomb repulsion. This is because electronic interactions suppress the quantum fluctuations between the degenerate bond-alternating phases, the alternation being maximized when the electronic kinetic and potential energies are approximately equal, namely when $U \sim 4t$.[32] For larger Coulomb interactions, however, charge degrees of freedom are effectively quenched and the EHP model maps to the spin-$\frac{1}{2}$ Heisenberg-Peierls chain with antiferromagnetic exchange[22] $J = 4t^2/(U - V)$. In this regime, virtual exchange[33] effectively lowers the barrier to resonance between the A and B phases, thereby reducing the dimerization and reconnecting with our earlier work,[15,17] and this is shown in Figs. 3 and 7.

The critical coupling, on the other hand, increases monotonically with U for both the Einstein- and Debye-phonon

TABLE I. Gap-crossing-determined bulk-limit values of $\beta(\gamma)$ and $\eta(\gamma)$ for $V = U/4 = t$. The value of g_c^∞ is shown for $\omega_\pi = t$. See Eq. (26).

γ	β	η	g_c^∞
1 (Einstein)	0.273	0.317	0.280
0.5	0.311	0.416	0.314
0 (Debye)	0.332	0.469	0.331

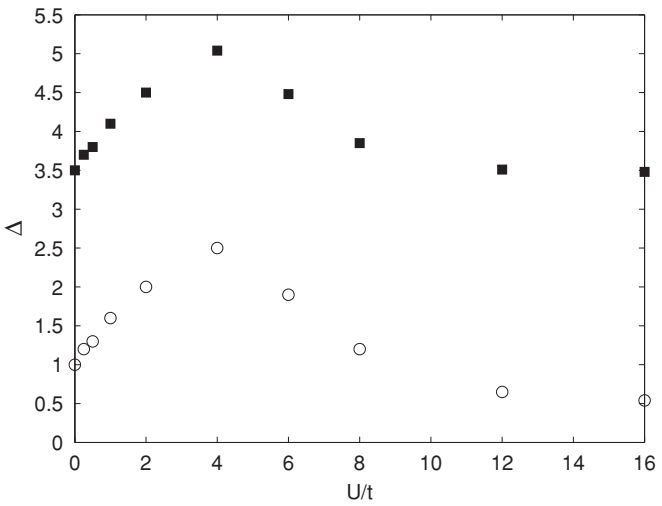

FIG. 3. Bulk spin gap Δ versus U/t for the infinite EHP chain for $\gamma = 1$ (Einstein) (squares); extrapolation to $\gamma = 0$ generates the Debye limit (circles). Δ is evaluated for $g = 4$, i.e., well into the Peierls phase. $\omega_\pi = V = U/4 = t$.

limits, contrasting with the behavior of the spin gap. The $U = 0$ intercept is found to be zero in both cases, as indicated in Fig. 4, in agreement with earlier work on the half-filled spinful SSH model.[18,22] The authors of Ref. 22 tentatively propose power-law scaling for the critical coupling $g_c^\infty \sim U^{0.3}$ for $V = U/4 = t$ and $\omega_\pi = t$, but cite the smallness of the spin gap as $(U,V) \to 0$ as a source of uncertainty below $U = 0.4t$. We note a similar power-law behavior,

$$g_c^\infty(U/t,\gamma) = \tilde{\beta}(\gamma)(U/t)^{\tilde{\eta}(\gamma)}, \tag{27}$$

which implies $g_c^\infty = 0\ \forall\ \omega_\pi$ when $U = 0$ in agreement with the earlier findings of Fradkin and Hirsch[18] and the many-body valence bond treatment of Dixit and Mazumdar.[32] The infinite-chain values of $\tilde{\beta}$ and $\tilde{\eta}$ are given in Table II.

B. Finite-size scaling

In order to ascertain the analytic behavior of the spin gap from the numerical data it is necessary to account for finite-size

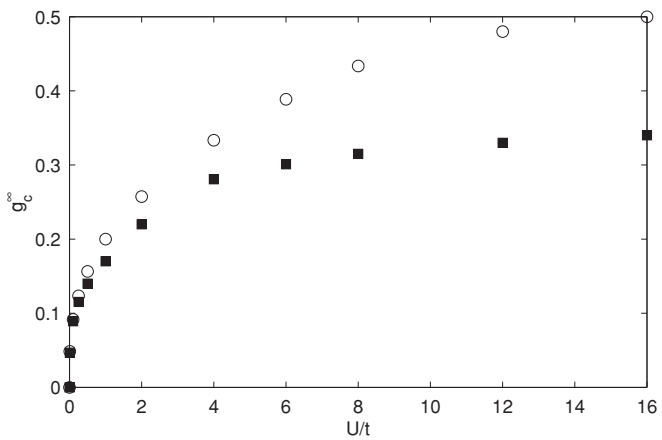

FIG. 4. Phase diagram in the g_c^∞-U plane for the infinite EHP chain for $\gamma = 1$ (Einstein) (squares); extrapolation to $\gamma = 0$ generates the Debye limit (circles). $\omega_\pi = V = U/4 = t$.

TABLE II. Gap-crossing-determined bulk-limit values of $\tilde{\beta}(\gamma)$ and $\tilde{\eta}(\gamma)$ for $\omega_\pi = V = U/4 = t$. See Eq. (27).

γ	$\tilde{\beta}$	$\tilde{\eta}$
1 (Einstein)	0.171	0.281
0.5	0.187	0.344
0 (Debye)	0.195	0.401

effects. We assume that the (singlet-triplet) gap $\Delta_N \equiv \Delta_{\rm st}$ for a finite system of N sites obeys the finite-size scaling hypothesis[34,35]

$$\Delta_N = \frac{1}{N} F(N\Delta_\infty), \tag{28}$$

with Δ_∞ the spin gap in the bulk limit. Recalling that $g_{\rm c}^\infty \equiv \lim_{N\to\infty} g_{\rm c}(N)$, it follows that $\Delta_\infty(g_{\rm c}^\infty) = 0$ and so curves of $N\Delta_N$ versus g are expected to coincide at the critical point where the bulk-limit spin gap vanishes. This is confirmed in Fig. 5 for the physical Debye limit (i.e., $\gamma = 0$). The critical value of g agrees very well with that found by the level crossing method (see Table I). As shown in Ref. 17, similar finite-size scaling exists for arbitrary γ in the Heisenberg-Peierls model, so we do not repeat the results here for arbitrary γ for the EHP model.

The finite-size scaling method is more robust than the gap-crossing approach, being applicable to the EHP Hamiltonian for all values of γ. On the other hand, its use as a quantitative method is limited by the accuracy with which plots may be fitted to Eq. (28). In practice, plots of $N\Delta_{\rm st}(N)$ versus g become progressively more kinked about the critical point as $\gamma \to 0$. Nevertheless, we find F to be well approximated by a rational function and the resulting $g_{\rm c}^\infty(\gamma)$ to be in accord with the predictions of the gap-crossover method.

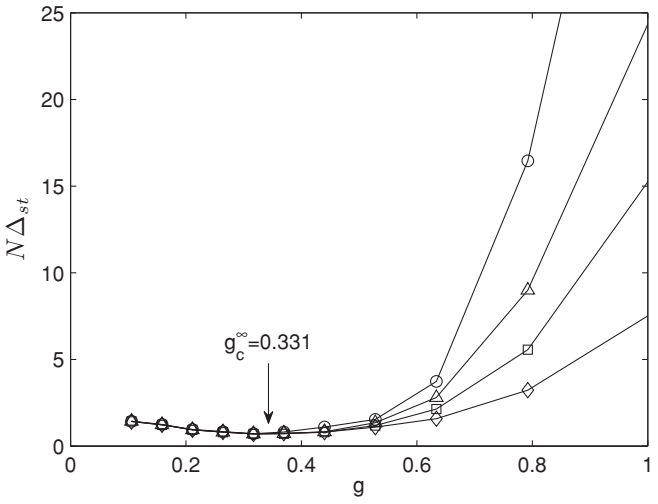

FIG. 5. $N\Delta_{\rm st}(N)$ versus the e-ph coupling g for the $\gamma = 0$ (Debye) EHP model for $N = 16$ (diamonds), 40 (squares), 100 (triangles), and 160 (circles). The curves converge at $g_{\rm c}$ (the value shown is obtained via gap crossing). $\omega_\pi = V = U/4 = t$.

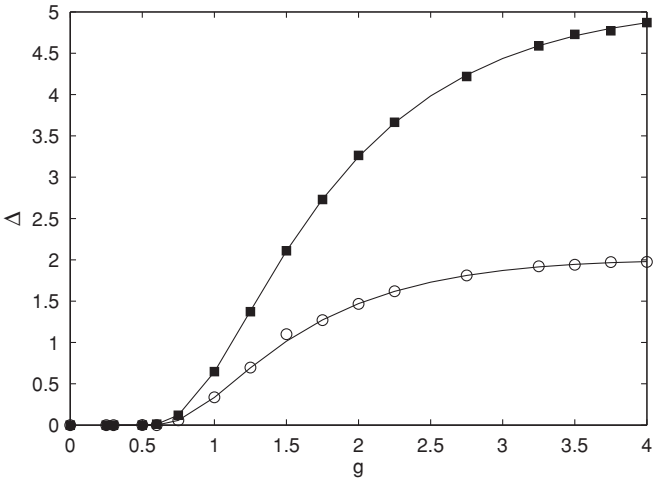

FIG. 6. Bulk-limit singlet-triplet gap Δ as a function of the e-ph coupling g with $\gamma = 1$ (Einstein) (squares) and $\gamma = 0$ (Debye) (circles) for $\omega_\pi = V = U/4 = t$. Plots are fitted to the BKT form [Eq. (29)].

C. Berezinskii-Kosterlitz-Thouless transition

For a BKT transition the spin gap $\Delta \equiv \lim_{N\to\infty} \Delta_{\rm st}$ is expected to exhibit an essential singularity at $g_{\rm c}^\infty$ with plots of $\Delta_{\rm st}$ versus g for $N \to \infty$ found to be well fitted by the Baxter form[36] (as shown in Fig. 6),

$$\Delta \sim a f(g) \exp\{-b[f(g)]^2\}, \tag{29}$$

where[11]

$$f(g) \equiv \left(g - g_{\rm c}^\infty\right)^{-1/2}. \tag{30}$$

Extrapolating $\Delta_{\rm st}(N)$ for $1/N \to 0$ generates Δ for a given γ and it is possible, in principle, to distinguish MI from PI GSs by examining the scaling behavior of $\Delta_{\rm st}(N)$, which tends to zero in the bulk limit for the critical MI and to a nonzero Δ for the gapped dimerized phase. However, not only must three parameters (a, b, and $g_{\rm c}^\infty$) be obtained from a nonlinear fit (shown in Table III), but there is considerable difficulty in determining Δ accurately near the critical point: the spin gap is extremely small even for values of g substantially higher than $g_{\rm c}^\infty$ due to the essential singularity in Eq. (29). Determining such small gaps from finite-size scaling is highly problematic, with very large lattices required to observe the crossover from the initial algebraic scaling (in the critical spin-sector regime) to exponential scaling (for gapped systems). Hence, the gap-crossover method is expected to be substantially more accurate than a fitting procedure for the determination of the critical coupling, the latter tending to overestimate $g_{\rm c}^\infty$,[11] as confirmed by a comparison of Tables I and III.

Finally, we consider the effect of Coulomb repulsions on the Baxter-equation parameters for which the corresponding plots are shown in Fig. 7. We note that the greatest amplitude Δ arises for $U \sim 4t$, in agreement with Sec. III A. For strong coupling, i.e., $U/t = 16$, the function approximates to that of the previously considered spin-Peierls model.[17] Beyond $U/t \approx 16$, the spinless-fermion picture becomes increasingly appropriate, in agreement with findings for the Hubbard model.[38]

TABLE III. Baxter-equation parameters obtained by fits to Eq. (29) for $\omega_\pi = V = U/4 = t$. The R^2 values are for a nonlinear least squares fitting, where $R^2 = 1$ means a totally correlated fit and $R^2 = 0$ means a totally uncorrelated fit (Ref. 37).

γ	a	b	g_c^∞	R^2
1 (Einstein)	18.501	2.521	0.285	0.971
0 (Debye)	6.704	2.091	0.349	0.973

D. Quantum bipartite entanglement

Entanglement has been shown to play an important role in the quantum phase transitions of interacting lattices. At the critical point—as in a conventional thermal phase transition—long-range fluctuations pervade the system. However, because the system is at $T = 0$, the nondegenerate GS is necessarily pure, indicating that the onset of (long-range) correlations is due to scale-invariant entanglement in the GS.

For an N-site lattice, bipartite entanglement is quantified through the von Neumann entropy,[39]

$$S(L = N/2, N) \equiv S_N = -\mathrm{Tr}_{\bar{S}} \rho_S(L) \log_2 \rho_S(L) = -\sum_\alpha \nu_\alpha \log_2 \nu_\alpha,$$

where $\rho_S(L)$ is the reduced-density matrix of an L-site block (typically coupled to an L-site environment $\bar{S}$ such that $2L = N$) and the ν_α are the eigenvalues of $\rho_S(L)$. Provided the entanglement is not too great and the ν_α decay rapidly, a matrix-product state is then a good approximation to the GS.[40]

Wu *et al.*[42] argued, quite generally, that QPTs are signaled by a discontinuity in some entanglement measure of the infinite quantum system. In Ref. 17 we demonstrated that the noncritical (gapped) phase entanglement is characterized by the saturation of the von Neumann entropy with increasing N, S_N growing monotonically until it is saturated for some block length N_0, in agreement with Ref. 43. The critical (gapless) phase, on the other hand, was found to exhibit logarithmic divergence in S_N at large N.

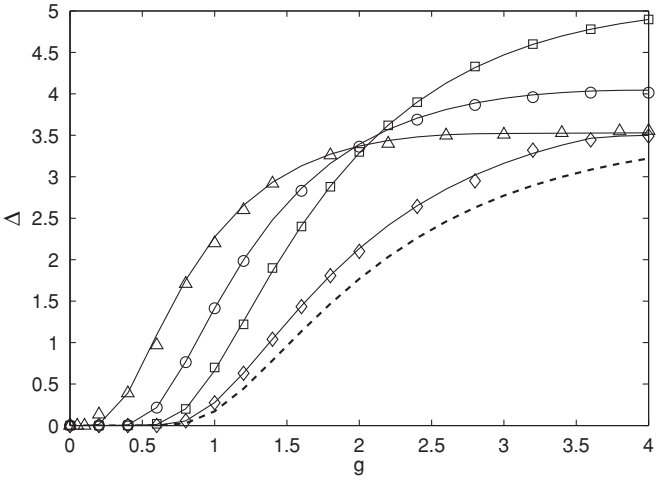

FIG. 7. Bulk-limit singlet-triplet gap Δ as a function of e-ph coupling g for $\gamma = 1$ (Einstein), $\omega_\pi = V = t$. $U/t = 0$ (triangles), t (circles), $4t$ (squares), and $16t$ (diamonds), and the Baxter-equation fitting for the spin-Peierls case (Ref. 17) ($U/t \to \infty$) (dashed line) are shown.

TABLE IV. Consistency of the various probes of the transition: Critical e-ph couplings determined by gap crossing (gap) and von Neumann entropy (vN) for $N = 20$, 40, and 80 sites for the Debye model ($\gamma = 0$). $\omega_\pi = V = U/4 = t$.

N	g_c^{gap}	g_c^{vN}
20	0.425	0.425
40	0.339	0.339
80	0.335	0.337

The principal difference between qubit lattices (e.g., spin chains) and itinerant-particle systems is the requirement of wave function antisymmetrization for indistinguishable fermions, which implies a Hilbert space lacking a direct-product structure. Such a structure may be recovered, however, by passing to the occupation number representation of local fermionic modes:[44] the N-site lattice is spanned by the 4^N states $\{\bigotimes_l |n\rangle_l\}$, where site l has local basis $\{|n\rangle_l\} = \{|0\rangle_l, |\uparrow\rangle_l, |\downarrow\rangle_l, |\uparrow\downarrow\rangle_l\}$. Under this formalism, the von Neumann entropy for pure states remains a well-defined entanglement measure, having been used to determine the phase diagram of the extended Hubbard model.[41]

For a given total system size N and phonon dispersion γ, the block entropy is found to be maximal for a nonzero spin-phonon coupling $g_c(N)$, close to the corresponding gap-crossing value (as shown in Table IV). As shown in Fig. 8, in the critical regime, $g < g_c(N)$, the block entropy is indeed found to scale logarithmically with system-block length, while in the gapped phase, $g > g_c(N)$, it is characterized by the emergence of a saturation length scale L_0 that varies with γ. These findings are in agreement with Ref. 43 and consistent with the observation that the transition belongs to the BKT universality class.[45]

E. Conformal invariance

Conformal field theory is a powerful means of characterizing the universality of a given 1D quantum field theory. In

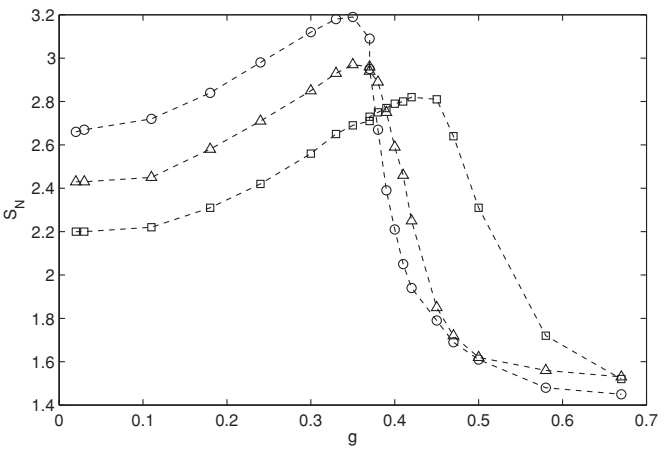

FIG. 8. Von Neumann entropy S_N for the $\gamma = 0$ (Debye) EHP model for lattice sizes $N = 20$ (squares), 40 (triangles), and 80 (circles); $L = N/2$. $\omega_\pi = V = U/4 = t$.

TABLE V. Finite-size computations of the conformal anomaly $c(N,N')$ and scaling dimension $x_{\rm st}(N,N')$ for the Debye model with $\omega_\pi = V = U/4 = t$, $g = 0.1$, and $N' = 20$.

N	$c(N,N')$	$x_{\rm st}(N,N')$
40	0.9928	0.4962
60	0.9970	0.4984
80	0.9984	0.4992
100	0.9990	0.4995
120	0.9993	0.4996

particular, the possible classes of critical behavior are indexed through a single dimensionless scalar, the central charge c of the underlying Virasoro algebra.[46] Furthermore, the finite-size corrections in the spectra of these models are closely related to the scaling dimensions of the primary fields O^α present in the theory, which in turn determine the critical exponents. The conformal anomaly is typically obtained from finite-size scaling,[47] viz.,

$$E_0(N) = N\epsilon_\infty - \frac{\pi v_\sigma c}{6N}, \tag{31}$$

where $E_0(N)$ is the GS energy for an N-site chain, v_σ is the model's spin-wave velocity, and ϵ_∞ is the bulk GS energy per site. In recent years, however, the central charge has been related to the entanglement entropy of a 1D critical system.[48] In particular, for a system of size N, the von Neumann entropy associated with a subsystem S of $L = N/2$ contiguous sites and reduced density matrix $\rho_S(L)$ is

$$S_N = \frac{c}{3}\ln\left(\frac{N}{\pi}\right) + c_1, \tag{32}$$

where c_1 is a nonuniversal constant. By considering two systems of respective size N and $N' \neq N$, Xavier[49] estimates the conformal anomaly $c(N,N')$ to be

$$c(N,N') = 3\left\{\frac{S_N - S_{N'}}{\ln(N/N')}\right\}. \tag{33}$$

For the critical regime, as shown in Table V for the Debye model, we obtain finite-size estimates of the conformal anomaly such that $c \to 1^-$.

For a system under periodic boundary conditions the structure of the higher-energy states is related to the scaling dimension x_α of the primary field to which the excitation pertains, i.e., O^α. An important result is the relation between the critical dimensions and the energy gaps of the finite-size system,[50]

$$E_\alpha(N) - E_0(N) = \frac{2\pi v_\sigma x_\alpha(N)}{N}, \tag{34}$$

where E_0 is the energy of the GS. With E_α as the energy of the lowest-lying triplet state, the finite-size relation in Eq. (31) gives

$$x_{\rm st}(N,N') = \frac{1}{12}\left\{\frac{\Delta_{\rm st}(N)c(N,N')}{N\epsilon_\infty - E_0(N)}\right\}. \tag{35}$$

As shown in Table V, we obtain $x_{\rm st} \to 1/2^-$, in agreement with RG analysis of finite-size behavior of the spin gap.[51,52]

F. Phase diagram

We now turn to a discussion of the phase diagram of the EHP model. Figure 2 shows the phase diagram as a function of the model parameters g and the $q = \pi$ phonon gap ω_π as defined in Eqs. (17) and (19). Evidently, for a fixed value of ω_π the Peierls state is less stable to dispersive, gapless quantum lattice fluctuations than to gapped, nondispersive fluctuations, implying that the $q < \pi$ phonons also destabilize the Peierls phase.

A qualitative explanation for this behavior proceeds as follows. The Peierls transition is accompanied by a divergence in the electronic susceptibility, which itself is accompanied by a divergence in the phonon self-energy[23] Σ_q. However, according to the definition that[23] $\Sigma_q \propto Mg^2\omega_q^2/K$ [and using Eq. (10) and Eq. (14)], we note that for a fixed optical gap the phonon self-energy in the Debye model is smaller than that of the Einstein model by a factor of $\sin(q/2)/\sqrt{2}$. Thus, the suppression of the Debye phonon self-energy with respect to the Einstein phonon self-energy suppresses the Peierls instability in the Debye model, and thus increases the critical electron-phonon coupling parameter.

It is also instructive to plot the phase diagram as a function of the *physical* parameters α and $\omega_b = \sqrt{K/M}$, as defined in Eqs. (2), (3) and (4). The mapping between model and physical parameters is achieved via Eqs. (10), (14), (24), and (25) (and setting $K = 1$). Since $\omega_\pi = \omega_b$ for the Einstein model, whereas $\omega_\pi = 2\omega_b$ for the Debye model, the Debye model is further into the antiadiabatic regime for a fixed value of ω_0. We also note that for a given model electron-phonon coupling parameter g the physical electron-phonon coupling parameter α is larger in the Debye model than the Einstein model [see Eqs. (10) and (14)]. Consequently, we expect the dimerized phase to be less robust to quantum fluctuations in the Debye model for fixed values of ω_b and α, as confirmed by Fig. 9.

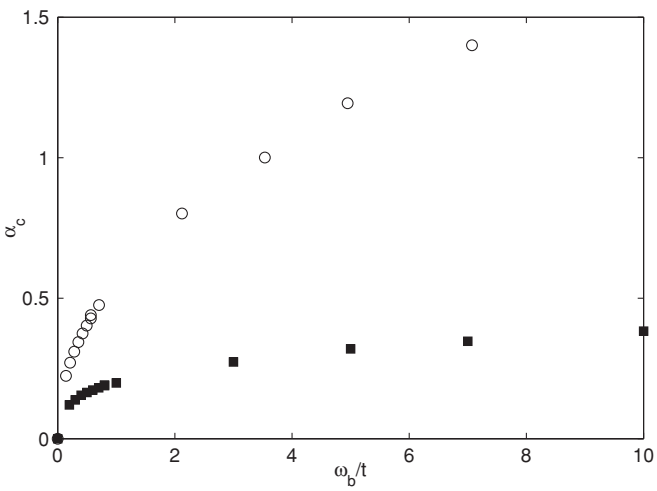

FIG. 9. Phase diagram in the α_c^∞-ω_b plane for the infinite EHP chain for $\gamma = 1$ (Einstein) (squares) and $\gamma = 0$ (Debye) (circles). $V = U/4 = t$.

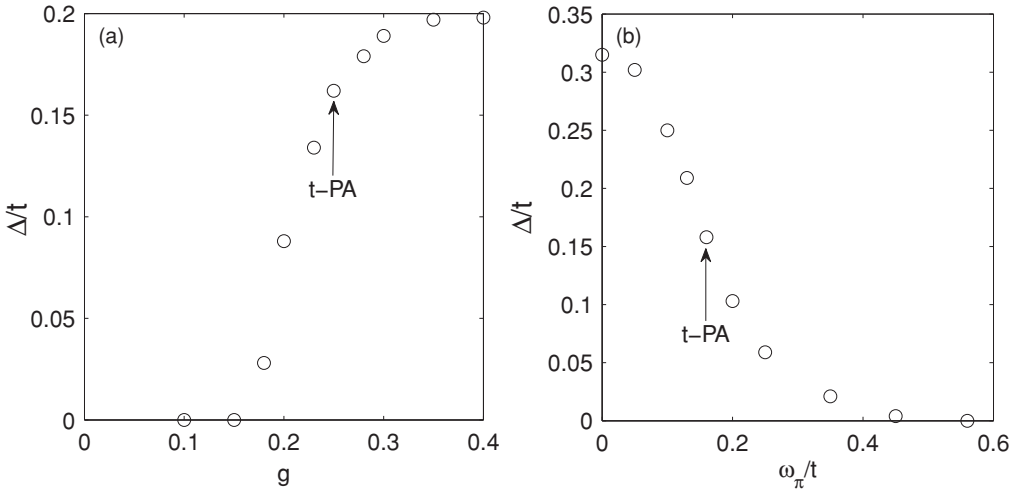

FIG. 10. Bulk-limit spin gap Δ (in units of t) for the EH-SSH model of t-PA as a function of (a) e-ph coupling, g (with $V = U/4 = t$ and $\omega_\pi = 0.158t$) and (b) phonon frequency ω_π/t (with $V = U/4 = t$ and $g = 0.253$).

G. Connection to spin-Peierls systems

Spin-Peierls chains with no net magentization, i.e., those for which $\sum_l S_l^z = 0$, map to half-filled pseudofermion-Peierls models under a Jordon-Wigner transformation. Using the renormalization group, the umklapp contribution to interfermion scattering is known to play a key role in the existence of a broken-symmetry GS, with the pseudoelectron-phonon coupling generating retarded backscattering (g_1) and umklapp ($g_3 = -g_1$) couplings; by virtue of the Pauli principle, however, the local character of the pseudofermion backscattering cancels out.[13] RG equations indicate that unless the nonlocal contribution to g_3 has both the right sign and bare initial value, the umklapp processes are irrelevant and the quantum system gapless. Conversely, if the threshold condition is satisfied, the umklapp processes and vertex function grow to infinity, signaling the onset of gapped excitations.

The spin gap in spinful fermionic systems, on the other hand, arises *because* of attractive overall backscattering, with the sign of g_1^T determining the existence (nonexistence) of an electronic Peierls GS.[24] The result of the commensurability effects arising from the relevance of the umklapp term for the half-filled band is the concurrent opening of a charge gap $\Delta^{(c)}$, separating the well-known Hubbard subbands. Coupling to quantized phonon degrees of freedom renormalizes both backward and umklapp terms.

Recapitulating the original treatment of Peierls for the half-filled band,[1] $U < 2V$ favors singly occupied lattice sites. In the Luttinger liquid phase, then, we have one electron per unit cell and lattice constant $a = \pi/2k_F$. For "small" U (and taking g to be critical), coupling to a distortion of wave vector $2k_F$ causes a spin gap to open spontaneously. The unit cell doubles in size $a \to a' = 2a$, accommodating two electrons. We have, then, that $a' = 2\pi/2k_F = \pi/k_F$, i.e., the reciprocal lattice vector and Fermi wave vector are coincident, opening a gap at the Fermi surface. Proceeding to the limit $U = \infty$, double occupancy is *prohibited*, which decouples spin and charge dynamics, effectively quenching the charge degrees of freedom and giving rise to an essentially filled valence band: $k_F^{U=\infty} = \pi/a$ and hence $k_F^{U=\infty} = 2k_F$. The system, under a JW transformation, maps to a spinless tight-binding fermion chain, i.e., one pseudoelectron per unit cell, the mapping generating an alternating real-space occupancy pattern reminscent of the $4k_F$ charge-ordered state in quarter-filled spin-1/2 systems. However, since the undistorted chain has one *pseudofermion* per unit cell, the system is half filled and umklapp scattering becomes relevant above a certain pseudoelectron-phonon-coupling threshold, opening a mass gap in the spectrum. Mapping the system back to a spin chain under an inverse

TABLE VI. Ground-state energy E_g/t of the EHP model as a function of the density-matrix eigenvalue product cutoff ϵ, number of system block states M, and superblock Hilbert space size (SBHSS) for a 32-site chain with $m_0 = 10$, $m_{\rm site} = 40$, $\gamma = 1$, and $\omega_\pi = V = U/4 = t$.

ϵ	E_g/t	M	SBHSS
10^{-10}	−54.2878527	872	57320
10^{-11}	−54.3284231	1034	91802
10^{-12}	−54.3364231	1026	164382
10^{-14}	−54.3376622	1118	412344
10^{-15}	−54.3376701	1056	582120

TABLE VII. Ground-state energy E_g/t and triplet gap $\Delta_{\rm st}/t$ for the EHP model as a function of the number of optimized *vibronic* levels per site $m_{\rm site}$. The number of bare phonon levels $m_0 = 10$, such that $m_{\rm site} = 40$ corresponds to no *in situ* optimization. $N = 32$ sites, $\epsilon = 10^{-14}$, $\gamma = 1$, and $\omega_\pi = V = U/4 = t$.

$m_{\rm site}$	M	E_g/t	$\Delta_{\rm st}/t$	SBHSS
10	954	−53.891822	0.330461	359782
14	1002	−54.258728	0.323939	398230
16	1028	−54.336620	0.323460	400286
18	1118	−54.337670	0.323450	412344
20	1124	−54.337683	0.323449	443234
30	1148	−54.337683	0.323448	469234
40	1124	−54.337684	0.323448	480322

TABLE VIII. As for Table VII, but with $N = 48$ sites.

m_{site}	M	E_g/t	Δ_{st}/t	SBHSS
10	954	−79.236943	0.232321	397788
14	1002	−79.877268	0.223939	408230
16	1028	−79.904964	0.217492	419232
18	1118	−79.905463	0.215678	430300
20	1124	−79.905571	0.214578	444090
30	1148	−79.905706	0.214583	489444
40	1124	−79.905710	0.214584	500356

JW transformation corresponds to a spin-gapped phase. In this way, we have a unified treatment of the electronic Peierls and spin-Peierls phases.

H. *trans-polyacetylene*

Electron-lattice and interelectron interactions in π-conjugated systems, such as *trans*-polyacetylene (*t*-PA), are conveniently modeled by the EHP chain for $\gamma = 0$, i.e., the extended Hubbard-SSH system (EH-SSH).[2,9,53] The low-energy electronic properties are dominated by a single, half-filled band involving the C_{2p_z} orbitals. π electrons, interacting via long-range Coulomb forces, are coupled to longitudinal phonons, with changes in bond length leading to linear corrections to the hybridization integrals. The interplay between the delocalization of the valence electrons and the associated local fluctuations of the Coulomb repulsion energy is fundamental in determining the dimerization of *t*-PA, which has been successfully described as a Mott-Peierls system by the EHP model.[9,53]

Dimerization in *t*-PA has also been studied in the adiabatic limit with the Pariser-Parr-Pople-Peierls model using the Ohno potential and the model parameters $t = 2.539$ eV, $U = 10.06$ eV, $\omega_0 = 0.2$ eV for C-C stretches, and the electron-phonon parameter $\lambda = 2\alpha^2/\pi Kt = 0.115$.[9,54] The relevant parameters for the EH-SSH model are then $\omega_\pi = 0.158t$, $V \approx U/4 \approx t$, and [using Eqs. (14) and (25)] $g_{t\text{-PA}} = 0.253$. The critical value of g for these parameters is $g_c = 0.140$.

The cross on Fig. 2 indicates *t*-PA's position in the phase diagram using these parameters. Figure 10 shows the spin gap versus an arbitrary value of g (with other parameters fixed) and an arbitrary value of ω_π (with other parameters fixed). Evidently, although the value of the bulk spin gap is close to its asymptotic value as function of g [see Fig. 10(a)], *t*-PA is close to the critical regime, resulting in large quantum fluctuations of the bond lengths.[7–9] We also see from Fig. 10(b) that the spin-gap value using the *t*-PA parameters (i.e., $\Delta_{\text{st}} \simeq 0.41$ eV) is approximately half the size of its adiabatic ($\omega_\pi \to 0$) value, in agreement with previous work using the full Pariser-Parr-Pople-Peierls model with quantum phonons.[9]

IV. CONCLUSIONS

The interplay between the repulsive, instantaneous Coulomb interactions and the attractive, retarded interactions mediated by phonons in a 1D tight-binding electron system results in competition between the Mott-insulator and Peierls-insulator ground states. For the extended Hubbard-Peierls chain the former becomes unstable with respect to lattice dimerization above a nonzero *e*-ph coupling threshold for all phonon gaps $\gamma\omega_\pi$. This observation is true for antiadiabatic phonons ($t/\omega_\pi \ll 1$) and remains applicable well into the adiabatic region of phonon phase space ($\omega_\pi/t < 1$).

Increasing the contribution of dispersive phonons to H_{ph} for fixed Coulomb interaction gives rise to a monotonic increase in the critical coupling for all Coulomb repulsions U, supporting the intuition that gapless phonons more readily penetrate the ground state (with the $q < \pi$ phonon modes renormalizing the dispersion at the Peierls-active modes). This observation has been corroborated by an array of independent verifications and is in agreement with our previous work on the spin Peierls chain.[17]

The DMRG method has also been used to analyze the effect of varying U/t from the noninteracting limit ($U/t = 0$) to the strongly correlated Heisenberg limit ($U/t \to \infty$), subject to $U = 4V$. For $U < 4t$ we observe an enhancement of the spin gap in the presence of repulsive interactions, with the dimerization being maximal for U approximately equal to the bandwidth. For larger U/t, the atomic charge fluctuations are severely reduced and the low-energy properties of the (quasilocalized) electrons are dominated by their spin degrees of freedom. The resulting spin-Peierls state is regarded as arising from the alternation of the strength of antiferromagnetic correlations between adjacent spins.

Finally, using the extended Hubbard model with Debye phonons, we investigated the Peierls transition in *trans*-polyacetylene and showed that the transition is close to the critical regime.

ACKNOWLEDGMENT

We thank Fabian Essler for discussions.

APPENDIX: DMRG CONVERGENCE

In situ optimization of the single-site basis is performed for the EHP model with m_0 oscillator levels per site, $M \sim 10^3$, and ca. 10^6 superblock states. In the absence of single-site optimization, the number of *vibronic* levels per site $m_{\text{site}} = d_{\text{site}} \times m_0$, where m_0 is the number of *oscillator* levels per site and d_{site} is the dimensionality of the electron subsector, i.e., $d_{\text{site}} = 4$ for the EHP model. Finite lattice sweeps are performed at target chain lengths under PBC. The convergence indicators are shown in Tables VI, VII, and VIII.

For confirmation of the convergence of the optimal-phonon DMRG for $\omega_\pi/t \sim 0.1$ [applicable to *trans*-polyacetylene (see Sec. III H)], we refer to the convergence tables in Ref. 9: for a 30-site chain, Δ_{st} is converged to within ± 0.001 eV for $m_0 = 5$ and $m_{\text{site}} = 18$. Since we intuitively expect a larger number of vibronic levels to be required for an accurate quantitative representation of the adiabatic regime, it is unsurprising to note excellent convergence for $m_{\text{site}} \sim 16$–18 when $\omega_\pi/t \sim 1$.

*william.barford@chem.ox.ac.uk

[1] R. Peierls, *Quantum Theory of Solids* (Oxford University Press, Oxford, 1955).

[2] D. Baeriswyl, D. K. Campbell, and S. Mazumdar, in *Conjugated Conducting Polymers*, edited by H. Kiess (Springer-Verlag, Berlin, 1992).

[3] W. Barford, *Electronic and Optical Properties of Conjugated Polymers* (Oxford University Press, Oxford, 2005).

[4] J. W. Bray, H. R. Hart, Jr., L. V. Interrante, I. S. Jacobs, J. S. Kasper, G. D. Watkins, S. H. Wee, and J. C. Bonner, Phys. Rev. Lett. **35**, 774 (1975).

[5] P. Monceau, *Electronic Properties of Inorganic Quasi One-Dimensional Compounds. Part II* (Reidel, Dordrecht, 1985).

[6] N. Tsuda, K. Nasu, A. Yanese, and K. Siratori, *Electronic Conduction in Oxides* (Springer-Verlag, Berlin, 1990).

[7] R. H. McKenzie and J. W. Wilkins, Phys. Rev. Lett. **69**, 1085 (1992).

[8] A. Weisse, H. Fehske, G. Wellein, and A. R. Bishop, Phys. Rev. B **62**, R747 (2000).

[9] W. Barford, R. J. Bursill, and M. Y. Lavrentiev, Phys. Rev. B **65**, 075107 (2002).

[10] M. Hase, I. Terasaki, and K. Uchinokura, Phys. Rev. Lett. **70**, 3651 (1993).

[11] R. J. Bursill, R. H. McKenzie, and C. J. Hamer, Phys. Rev. Lett. **83**, 408 (1999).

[12] E. Jeckelmann, C. Zhang, and S. R. White, Phys. Rev. B **60**, 7950 (1999).

[13] L. G. Caron and S. Moukouri, Phys. Rev. Lett. **76**, 4050 (1996).

[14] R. Citro, E. Orignac, and T. Giamarchi, Phys. Rev. B **72**, 024434 (2005).

[15] W. Barford and R. J. Bursill, Phys. Rev. Lett. **95**, 137207 (2005).

[16] K. Kuboki and H. Fukuyama, J. Phys. Soc. Jpn. **56**, 3126 (1987).

[17] C. J. Pearson, W. Barford, and R. J. Bursill, Phys. Rev. B **82**, 144408 (2010).

[18] E. Fradkin and J. E. Hirsch, Phys. Rev. B **27**, 1680 (1983).

[19] The spinless model, on the other hand, has a disordered phase for small coupling if M is finite, with an ordered phase realized for bare coupling in excess of a certain threshold. As $M \to \infty$ the size of the disordered region shrinks to zero, reconnecting with the adiabatic result of Peierls and Frölich (Ref. 1).

[20] E. H. Lieb and F. Y. Wu, Phys. Rev. Lett. **20**, 1445 (1968).

[21] P. Sengupta, A. W. Sandvik, and D. K. Campbell, Phys. Rev. B **65**, 155113 (2002).

[22] P. Sengupta, A. W. Sandvik, and D. K. Campbell, Phys. Rev. B **67**, 245103 (2003).

[23] E. von Oelsen, A. Di Ciolo, J. Lorenzana, G. Seibold, and M. Grilli, Phys. Rev. B **81**, 155116 (2010).

[24] G. T. Zimanyi, S. A. Kivelson, and A. Luther, Phys. Rev. Lett. **60**, 2089 (1988); G. T. Zimanyi and S. A. Kivelson, Mol. Cryst. Liq. Cryst. **160**, 457 (1988).

[25] C. Zhang, E. Jeckelmann, and S. R. White, Phys. Rev. B **60**, 14092 (1999).

[26] H. Fukutome and M. Sasai, Prog. Theor. Phys. **67**, 41 (1982).

[27] G. Wellein, H. Fehske, and A. P. Kampf, Phys. Rev. Lett. **81**, 3956 (1998).

[28] S. R. White, Phys. Rev. Lett. **69**, 2863 (1992); Phys. Rev. B **48**, 010345 (1993).

[29] W. Barford and R. J. Bursill, Phys. Rev. B **73**, 45106 (2006).

[30] See, for example, C. Kittel, *Quantum Theory of Solids* (Wiley, New York, 1987), p. 25.

[31] K. Okamoto and K. Nomura, Phys. Lett. A **169**, 433 (1992).

[32] S. N. Dixit and S. Mazumdar, Phys. Rev. B **29**, 1824 (1984).

[33] P. W. Anderson, Phys. Rev. **79**, 350 (1950).

[34] M. E. Fisher and M. N. Barber, Phys. Rev. Lett. **28**, 1516 (1972).

[35] C. J. Hamer and M. N. Barber, J. Phys. A **14**, 241 (1981).

[36] R. J. Baxter, J. Phys. C **6**, L94 (1973).

[37] J. Freese and J. S. Long, *Regression Models for Categorical Dependent Variables Using Stata* (Stata Press, College Station, 2006).

[38] H. J. Schulz, Phys. Rev. Lett. **64**, 2831 (1990).

[39] C. H. Bennett, H. J. Bernstein, S. Popescu, and B. Schumacher, Phys. Rev. A **53**, 2046 (1996).

[40] U. Schollwock, Rev. Mod. Phys. **77**, 259 (2005).

[41] C. Mund, Ö. Legeza, and R. M. Noack, Phys. Rev. B **79**, 245130 (2009).

[42] L.-A. Wu, S. Bandyopadhyay, M. S. Sarandy, and D. A. Lidar, Phys. Rev. A **72**, 032309 (2005).

[43] G. Vidal, Phys. Rev. Lett. **99**, 220405 (2007).

[44] P. Zanardi, Phys. Rev. A **65**, 042101 (2002).

[45] J. M. Kosterlitz and D. J. Thouless, J. Phys. C **6**, 1181 (1973).

[46] A. A. Belavin, A. M. Polyakov, and A. B. Zamolodchikov, Nucl. Phys. B **241**, 333 (1984).

[47] H. W. J. Blöte, J. L. Cardy, and M. P. Nightingale, Phys. Rev. Lett. **56**, 742 (1986).

[48] For a review see, P. Calabrese and J. Cardy, J. Phys. A **42**, 504005 (2009).

[49] J. C. Xavier, Phys. Rev. B **81**, 224404 (2010).

[50] J. L. Cardy, J. Phys. A **17**, L385 (1984).

[51] M. Nakamura, A. Kitazawa, and K. Nomura, Phys. Rev. B **60**, 7850 (1999).

[52] In Ref. 51 $x_{\rm st}(N) = [2 - y_0/(y_0 \ln N + 1)]/4$, where $y_0 \sim g_1^T/(\pi v_\sigma)$.

[53] E. Jeckelmann, Phys. Rev. B **57**, 11838 (1998).

[54] R. J. Bursill and W. Barford, Phys. Rev. Lett. **82**, 1514 (1999); W. Barford, R. J. Bursill, and M. Y. Lavrentiev, Phys. Rev. B **63**, 195108 (2001).